

Pulsar motions in our Galaxy

X. H. Sun and J. L. Han

National Astronomical Observatories, Chinese Academy of Sciences, Beijing 100012, China
xhsun@bao.ac.cn (XHS), hjl@bao.ac.cn (JLH)

Accepted

; Received

ABSTRACT

Pulsar motions in our Galaxy from their birth until 2 Gyr are studied statistically via Monte-Carlo simulation of 2×10^5 pulsars with the best available representation of the Galactic potential. We find that the distribution of height above the Galactic plane for pulsars with characteristic ages less than about 8 Myr could be well fitted by a Gaussian function. For older pulsars, an extra exponential function is necessary to fit the distribution. The scale-height of the Gaussian component increases linearly with time until about 40 Myr. The height distribution becomes stabilized after about 200 Myr. These results are not sensitive to initial height or radial distributions. Taking the relationship between the initial velocity and height distribution, we found from the latest pulsar catalog that the height distribution of pulsars younger than 1 Myr directly implies the mean initial velocity of $280 \pm 96 \text{ km s}^{-1}$. Comparison of simulated sample of pulsars with the current available millisecond pulsars shows that their 1D initial velocity dispersion should be most probably $60 \pm 10 \text{ km s}^{-1}$.

Key words: pulsar: general

1 INTRODUCTION

Pulsars are high velocity objects in our Galaxy (Lyne & Lorimer 1994). They were born in supernova explosions near the Galactic plane where their progenitors live, but move away very fast from the plane. The evolution of pulsar heights was considered (Bhattacharya et al. 1992; Hartman et al. 1997; Mukherjee & Kembhavi 1997) but not explicitly described in most pulsar population syntheses, therefore, the picture for pulsar height evolution was not very clear. We want to demonstrate in this paper by 3D simulations how pulsars move in our Galaxy.

Birth velocities of both normal and millisecond pulsars (MSPs) have been investigated by many authors. For normal pulsars, Lyne & Lorimer (1994) studied transverse speeds of 29 pulsars younger than 3 Myr and obtained the mean birth velocity $\bar{V}_B = 450 \pm 90 \text{ km s}^{-1}$. Taking into account selection effects and using all available pulsar proper motion data in population synthesis, Lorimer, Bailes & Harrison (1997) found the mean birth velocity $\bar{V}_B \sim 500 \text{ km s}^{-1}$. Hansen & Phinney (1997) considered the distribution of proper motions, including all available upper limits, and concluded that the mean birth velocity \bar{V}_B should be smaller, only 250–300 km s^{-1} . Cordes & Chernoff (1998) performed a detailed analysis for measured velocities of 49 young pulsars. They favoured a two-component Gaussian model in 3-dimension with characteristic velocities* σ_v of 175 km s^{-1}

and 700 km s^{-1} . Arzoumanian, Chernoff & Cordes (2002) infer the velocity distribution of radio pulsars detected in 400-MHz surveys, taking into account beaming, selection effects and luminosity evolution. They also favour a two-component Gaussian model with $\sigma_v \sim 90 \text{ km s}^{-1}$ and 500 km s^{-1} .

For MSPs, Lorimer (1995) accounted for known survey selection effects and obtained the local surface density of MSPs, birthrate and the lower limit of the mean birth velocity that is $\sigma_v > 50 \text{ km s}^{-1}$, i.e. $\bar{V}_B \geq 80 \text{ km s}^{-1}$. The results were confirmed by Cordes & Chernoff (1997), who obtained the velocity perpendicular to the Galactic plane, $v_z = 52^{+17}_{-11} \text{ km s}^{-1}$, i.e. a 3-D velocity dispersion $\sigma_v = 84 \text{ km s}^{-1}$ using likelihood analysis on previous surveys for MSPs plus selection effects. Later, Lyne et al. (1998) found that the population syntheses of the MSPs with the Maxwellian initial 1D velocity dispersion of $80 \pm 20 \text{ km s}^{-1}$ agrees the best with the data of newly discovered MSPs in Parkes southern sky survey together with previous MSPs. The 3D mean birth velocity is correspondingly $130 \pm 30 \text{ km s}^{-1}$. These results were later confirmed by Toscano et al. (1999) using more MSP proper motions obtained from timing measurements.

Previously, Narayan & Ostriker (1990) tried to model the observed pulsar populations. They deduced an analytic formula for the height distribution by assuming a Gaussian distribution at all times and solving the energy conserva-

* In the Maxwellian distribution, velocity in each dimension is

a Gaussian distribution. The mean velocity in 3-D and velocity dispersion in 1-D are connected by $\bar{V}_B \sim \sigma_v \sqrt{8/\pi} \simeq 1.6\sigma_v$.

tion equation in z -direction (perpendicular to the Galactic plane). However, the height distribution changes from time to time when pulsars run away from the Galactic plane. The integrated z -distribution of pulsars with different ages may not be a Gaussian. We will show by our Monte-Carlo simulation that the scale-height evolution is much more complicated than a Gaussian. Analytic solutions obtained from the over-simplified form of a Galactic acceleration model can hardly represent the realistic situation, especially over long time with non-linear evolution of pulsar heights. By simulations, we are able to track the height distribution of a pulsar sample, for any form of acceleration.

In our work, the initial velocity dispersion for MSPs is obtained by comparison of the height distribution between simulated and observed pulsar samples. We also tried to derive the initial velocity dispersion of normal pulsars by comparing their scale-heights and characteristic ages. In Section 2 we will describe the simulation procedures together with input parameters and governing equations. Several possibilities of parameter choice are also discussed. In Section 3, we show the simulation results, mostly regarding how the pulsar scale-height evolves. We demonstrate in Section 4 two applications of our simulations, i.e. to determine the birth velocity dispersions of normal pulsars and MSPs. The influence of the selection effects is also discussed. The conclusions are given in Section 5.

2 DETAILS OF SIMULATION

In our simulations, we take a Galactocentric rectangular coordinate system, where the x and y -axes are orthogonal in the Galactic plane and z -axis perpendicular to the plane. The dynamic status of a pulsar at any time can be described by $(x, y, z; v_x, v_y, v_z)$, where x , y and z are position coordinates, and v_x , v_y and v_z the velocities along each axis. Obviously, the Galactocentric radius $R = \sqrt{x^2 + y^2}$. The distance between the Sun and the Galactic center is taken as $R_0 = 8.0$ kpc. Simulation results should not depend on coordinate system taken. Before calculating pulsar positions at any time t , the initial positions and velocities of pulsars and the Galactic acceleration should be discussed.

2.1 Initial height distribution

Initial positions of pulsars should follow the positions of their progenitors, e.g. OB stars, or the distribution of supernova remnants. Maíz-Apellániz (2001) has listed all previous determinations of scale heights of the OB star disk in either an exponential or a Gaussian height distribution. He obtained a solid measurement of the vertical distribution of B-B5 stars in solar neighborhood as

$$P_z(z_{\text{ini}}) = \frac{1}{\sqrt{2\pi}h_{\text{ini}}} \exp\left(-\frac{z_{\text{ini}}^2}{2h_{\text{ini}}^2}\right) \quad (1)$$

with a scale-height of $h_{\text{ini}} = 63$ pc from *Hipparcos* data, though a single-component, self-gravitating, and isothermal disk model with a *sech* function is as good as the Gaussian. Here we ignore the halo component which is about 4% of stars, and it is not clear whether this component is related to MSPs. In our simulations, we assume this height distribution to be adequate for any places in the disk.

We also tried an exponential distribution $P_z(z_{\text{ini}}) = (1/2h_{\text{ini}}) \exp(-|z_{\text{ini}}|/h_{\text{ini}})$ with a scale-height $h_{\text{ini}} = 60$ pc and a flat distribution in infinitely thin disk ($z_{\text{ini}} = 0$). We found that *our results are not sensitive to different initial z -distributions*, as all of them lead to the same or very similar dynamic behavior after one million year. In the following we will use the Gaussian distribution in Eq.(1), and assume it is valid at all Galactocentric radii.

2.2 Initial radial distribution

The radial density distribution of newly born neutron stars is not clear at all. Narayan (1987) made a Gaussian fit to the observed radial density profile obtained by Lyne, Manchester & Taylor (1985) as using a normalized function

$$\rho_R(R) = \frac{1}{64\pi} \exp\left[-\left(\frac{R}{8}\right)^2\right] (\text{kpc})^{-2}, \quad (2)$$

where ρ_R is radial density. Bailes & Kniffen (1992) pointed out that another function with $\rho_R \rightarrow 0$ as $R \rightarrow 0$ is also consistent with the observed data. However, most of the subsequent work took Narayan's fit as a starting distribution in R (e.g. Lorimer et al. 1993; Johnston 1994; Mukherjee & Kembhavi 1997). While, this distribution reflects the observed distribution in R , rather than the initial distribution which most probably is related to the exponential distribution of OB stars in the Galactic plane, as expected in our Galaxy and other spiral galaxies (Bahcall 1986; Paczyński 1990). Note here that *the radial probability distribution* (P_R), which is used for discussions below and plots in Figure 1, should have the form of

$$P_R dR = \frac{2\pi R \rho_R dR}{\int_0^\infty 2\pi R \rho_R dR}. \quad (3)$$

For Narayan's function[†], $P_R = \frac{R}{32} \exp\left[-\left(\frac{R}{8}\right)^2\right]$. In fact, this function has a natural deficit for $R \rightarrow 0$ which can be evidently seen from the observed data that Johnston (1994) tried to explain.

In our simulations, we have tested a few probability functions, as shown in Figure. 1.

(1) *The exponential distribution:*

$$P_R(R_{\text{ini}}) = \frac{1}{R_{\text{exp}}} \exp\left(-\frac{R_{\text{ini}}}{R_{\text{exp}}}\right), \quad (4)$$

hereafter $R_{\text{ini}} = \sqrt{x_{\text{ini}}^2 + y_{\text{ini}}^2}$ is the initial Galactocentric radius. The re-scaled characteristic radius $R_{\text{exp}} = 4.7$ kpc[‡], as given in Hartman et al.(1997);

(2) *The Gamma distribution:*

$$P_R(R_{\text{ini}}) = a_R \frac{R_{\text{ini}}}{R_{\text{exp}}^2} \exp\left(-\frac{R_{\text{ini}}}{R_{\text{exp}}}\right), \quad (5)$$

with $R_{\text{exp}} = 4.5$ kpc and $0.4 \text{ kpc} \leq R_{\text{ini}} \leq 25$ kpc following Paczyński (1990). This radial distribution corresponds

[†] We note that in literature some authors claimed to use the Gaussian radial distribution of Narayan (1987), but as a mistake, they used the form of $\rho_R(R)$ to represent P_R . The prefactor of P_R , $R/32$, is R dependent, while that of $\rho_R(R)$ is a constant of $1/(64\pi)$.

[‡] The authors implicitly used $R_0 = 8.5$ kpc in context. Here we scaled it to $R_0 = 8.0$ kpc. Same are the following cases 3, 4.

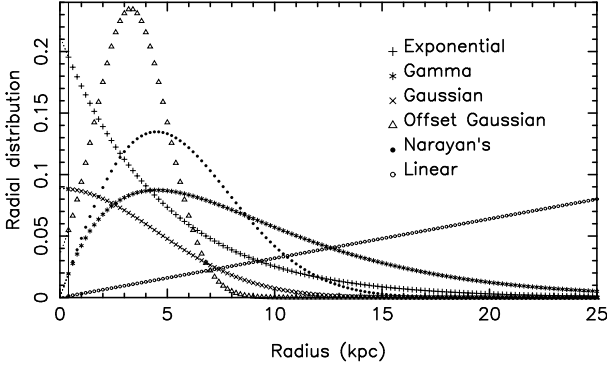


Figure 1. Different forms of radial distribution plotted against radius R . A uniform density distribution is a linearly increasing function P_R against R . The vertical line at $R = 0.4$ kpc indicates the minimum R in our simulation.

to exponential radial density. Here $a_R = 1.0683$. See also Gonthier et al. (2002);

(3) *The Gaussian distribution,*

$$P_R(R_{\text{ini}}) = \frac{1}{\sqrt{2\pi}R_g} \exp\left(-\frac{R_{\text{ini}}^2}{2R_g^2}\right), \quad (6)$$

with a rescaled $R_g = 4.5$ kpc following Lorimer et al. (1993). Many authors (e.g. Hartman et al. 1997) used this distribution afterwards;

(4) *The offset Gaussian distribution:*

$$P_R(R_{\text{ini}}) = \frac{1}{\sqrt{2\pi}R_g} \exp\left[-\frac{(R_{\text{ini}} - R_{\text{off}})^2}{2R_g^2}\right], \quad (7)$$

with rescaled $R_g = 1.7$ kpc and $R_{\text{off}} = 3.3$ kpc given by Hartman et al. (1997);

(5) *The distribution from Narayan:*

$$P_R(R_{\text{ini}}) = \frac{R_{\text{ini}}}{R_g^2} \exp\left(-\frac{R_{\text{ini}}^2}{2R_g^2}\right) \quad (8)$$

here $R_g = 4.5$ kpc taken from the normalized factor of the Gaussian distribution;

(6) *The linear distribution:*

$$P_R(R_{\text{ini}}) = \frac{2R_{\text{ini}}}{R_2^2 - R_1^2} \quad (9)$$

so that in a given range of Galactocentric radii $R_1 < R_{\text{ini}} < R_2$ (we took $R_1 = 0.4$ kpc and $R_2 = 25$ kpc) the pulsar surface density to be a constant.

We have simulated pulsar motions in all above cases and will make comparison on the evolved radial distribution, while for detailed studies, we will concentrate on the Gamma distribution (Eq. 5).

2.3 Initial velocities

The initial velocities can be written as $\vec{v}_{\text{ini}} = \vec{v}_{\text{birth}} + \vec{v}_{\text{rot}}$, where \vec{v}_{birth} is the birth velocity and \vec{v}_{rot} the rotation velocity of the Galaxy. The physical origin of the birth velocity is not clear hitherto, which might be generated from the disruption of a binary (Gunn & Ostriker 1970), rocket effects (Helfand & Tademaru 1977) or asymmetric supernova explosion (Dewey & Cordes 1987). We will not go further

into details but assume that the birth velocity is isotropic and follows a Maxwellian distribution

$$P_v(v_{\text{birth}}) = \sqrt{\frac{2}{\pi}} \frac{v_{\text{birth}}^2}{\sigma_{\text{birth}}^3} \exp\left(-\frac{v_{\text{birth}}^2}{2\sigma_{\text{birth}}^2}\right), \quad (10)$$

where σ_{birth} is 1D velocity dispersion, corresponding to the mean velocity of $\sqrt{8/\pi}\sigma_{\text{birth}}$ or a 3D velocity dispersion of $\sqrt{3}\sigma_{\text{birth}}$. We will show the dynamical results of $\sigma_{\text{birth}} = 100, 200, 300$ and 400 km s⁻¹ in our simulations[§].

2.4 Galactic potential and acceleration

Pulsars accelerate in the Galactic gravitational potential, as the acceleration being $\vec{g} = -\nabla\phi$. The potential ϕ is determined by the mass distribution in our Galaxy, $\nabla^2\phi = 4\pi G\rho$, where G is the gravitational constant, and ρ mass density as a function of position. One can find that

$$\nabla \cdot \vec{g} = -4\pi G\rho \quad (11)$$

In fact, Eq. 11 can be rewritten as

$$\rho = -\frac{1}{4\pi G} \left\{ \frac{\partial g_z}{\partial z} + \frac{1}{R} \frac{\partial (R g_R)}{\partial R} \right\} \quad (12)$$

in a cylindrical coordinate system. Here g_z is the acceleration in z direction and g_R in R direction. In order to simulate pulsar dynamics, it is very important to find the best representation of the Galactic potential.

2.4.1 Adopted Galactic potential model

We used the potential model of disk/bulge originally proposed by Miyamoto & Nagai (1975),

$$\phi_i(R, z) = \frac{GM_i}{\left\{ R^2 + \left[a_i + (z^2 + b_i^2)^{1/2} \right]^2 \right\}^{1/2}}, \quad (13)$$

here a_i, b_i and M_i are model parameters, and $i = 1$ stands for the bulge and $i = 2$ for the disk. Using the density distribution of the halo given by Kuijken & Gilmore (1989),

$$\rho = \frac{\rho_c}{1 + (r/r_c)^2}. \quad (14)$$

here $r^2 = x^2 + y^2 + z^2$, Paczyński (1990) derived the potential for the halo component as

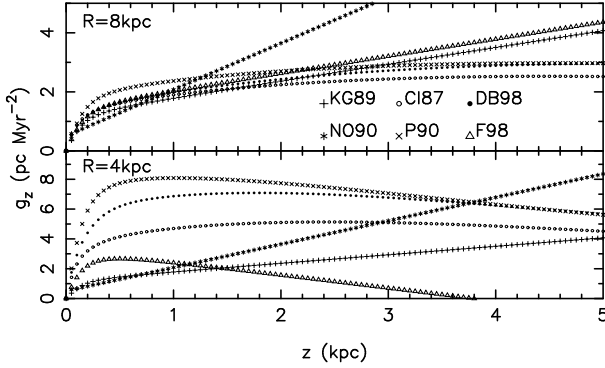
$$\phi_h = -\frac{GM_c}{r_c} \left[\frac{1}{2} \ln \left(1 + \frac{r^2}{r_c^2} \right) + \frac{r_c}{r} \operatorname{atan} \frac{r}{r_c} \right], \quad (15)$$

where $M_c = 4\pi\rho_c r_c^3$ and ρ_c and r_c are model parameters. Paczyński (1990) determined all the parameters (see Table 1) for the disk, bulge and halo potentials to make a good agreement with the rotation curve, local volume density and the column density between $z = \pm 700$ pc. He took $R_0 = 8.0$ kpc. This potential expression has been used for simulations of pulsar motions by Hansen & Phinney (1997), Cordes & Chernoff (1998) and Gonthier et al. (2002). Since the rotation curve for $R < 0.4$ kpc can not be well described by the formula of the potentials, as Sofue & Rubin (2001) show, all our simulations have been limited to $R > 0.4$ kpc.

[§] Note here $1 \text{ km s}^{-1} \approx 1 \text{ pc Myr}^{-1}$.

Table 1. Potential parameters given by Paczyński (1990) with subscripts 1 and 2 corresponding to bulge and disk and c to halo.

a_1 (kpc)	0
b_1 (kpc)	0.277
M_1 (M_\odot)	1.12×10^{10}
a_2 (kpc)	3.7
b_2 (kpc)	0.20
M_2 (M_\odot)	8.07×10^{10}
r_c (kpc)	6.0
M_c (M_\odot)	5.0×10^{10}

**Figure 2.** Acceleration g_z calculated for $R = 4$ kpc and 8 kpc for the models by Carlberg & Innanen (1987: CI87), Dehnen & Binney (1998: DB98), Ferrière (1998: F98), Kuijken & Gilmore (1989: KG89), Narayan & Ostriker (1990: NO90) and Paczyński (1990: P90).

2.4.2 Galactic potential previously used

Previously, several models for Galactic mass distribution and 1D acceleration have been used to simulate pulsar motions in the z -direction.

1. Narayan & Ostriker (1990) modeled the mass density in the Galaxy as a thin layer at $z = 0$ with surface density Σ and a uniform halo with density of ρ , and obtained the acceleration in z -direction as,

$$g_z = 4\pi G\rho \left[z + \frac{\Sigma}{2\rho} \frac{|z|}{z} \right]. \quad (16)$$

This model was also used by Itoh & Hiraki (1994) and tried by Hartman & Verbunt (1995).

2. Kuijken & Gilmore (1989) rewrote Eq.(12) as

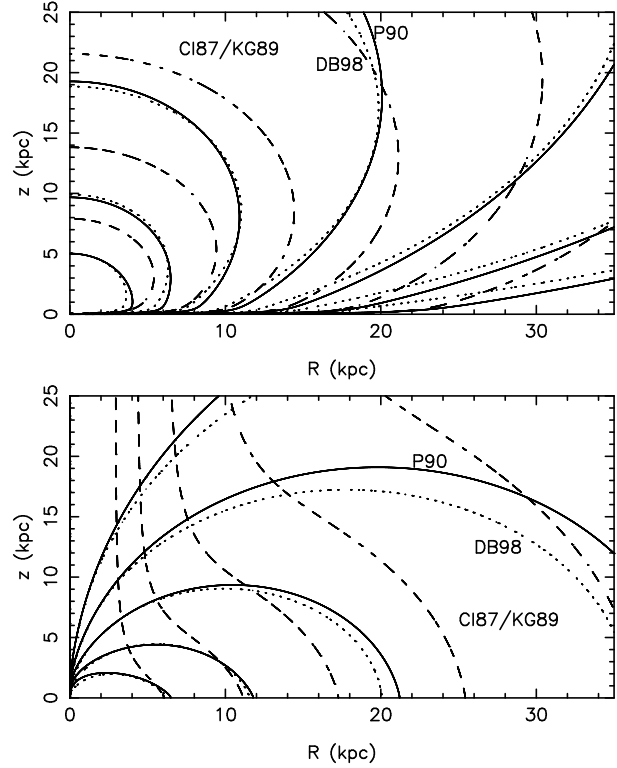
$$\rho = -\frac{1}{4\pi G} \left\{ \frac{\partial g_z}{\partial z} + 2(A^2 - B^2) \right\} \quad (17)$$

for disk galaxies following Mihalas & Binney (1981). Here A and B are the Oort constants. After considering the double-exponential disks and the spherical components (halo, bulge and corona), they modeled the distribution of matter in the disk via tracer stars at high z and obtained the acceleration in z -direction

$$g_z = 1.04 \times 10^{-3} \left(\frac{1.26z}{\sqrt{z^2 + 0.18^2}} + 0.58z \right) \quad (18)$$

which can be further used to determine the disk surface density.

Their formula of g_z has been used by Bhattacharya et al. (1992) and Hartman & Verbunt (1995) to simulate

**Figure 3.** The contours of g_z (upper panel) and g_R (lower panel) calculated from potentials of Dehnen & Binney (1998: DB98), Paczyński (1990: P90), and Carlberg & Innanen (1987) with modified parameters by Kuijken & Gilmore (1989: CI87/KG89). The contour levels are at 2^n pc Myr $^{-2}$, with $n = 0, \pm 1, \pm 2, \pm 3$, and with notes near $n=0$.

the pulsar motions in z -directions for investigation of pulsar magnetic field decay, and extended by Ferrière (1998) for ISM distribution studies. It seems to have been much better constrained at high z than that of Narayan & Ostriker (1990). See Figure 2 and discussions by Hartman & Verbunt (1995).

3. The potential model for the disk/spheroid and nucleus/bulge, either directly from Carlberg & Innanen (1987) or using parameters given by Kuijken & Gilmore (1989), has the form of

$$\phi_{dh} = \frac{GM}{\left\{ \left[a + \sum_{i=1}^3 \beta_i (z^2 + h_i^2)^{1/2} \right]^2 + b^2 + R^2 \right\}^{1/2}}, \quad (19)$$

$$\phi_{b,n} = \frac{GM_{b,n}}{(b_{b,n}^2 + R^2)^{1/2}}, \quad (20)$$

which has been used by Lorimer et al. (1993, 1997), Hartman et al. (1997) and Mukherjee & Kembhavi (1997) for pulsar population synthesis. The model parameters a , b , h_i , β_i and mass M for different components were constrained by the rotation curve data.

4. Dehnen & Binney (1998) have constructed a set of mass models for our Galaxy using all available observational constraints. All of their models consist of the spheroidal bulge, halo and three disk components, namely the thin and thick stellar disks and the interstellar medium disk. The

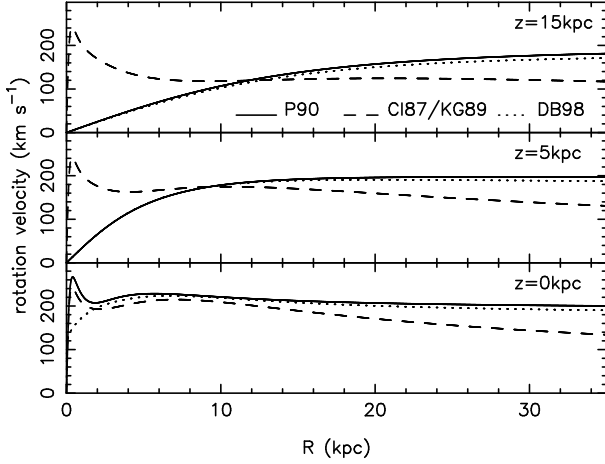


Figure 4. The rotation curves at different z from the mass models of Dehnen & Binney (1998: DB98), Paczyński (1990: P90), and Carlberg & Innanen (1987) with modified parameters by Kuijken & Gilmore (1989: CI87/KG89).

density for bulge and halo in the model is described by the spheroidal density distribution

$$\rho_s = \rho_0 \left(\frac{m}{r_0}\right)^{-\gamma} \left(1 + \frac{m}{r_0}\right)^{\gamma-\beta} \exp(-m^2/r_t^2). \quad (21)$$

Here $m = (R^2 + q^{-2}z^2)^{1/2}$, and the density of disks is given by

$$\rho_d(R, z) = \frac{\Sigma_d}{2z_d} \exp\left(-\frac{R_m}{R_d} - \frac{R}{R_d} - \frac{|z|}{z_d}\right), \quad (22)$$

where ρ_0 , r_0 , q , γ , β , r_t , Σ_d , z_d , R_d and R_m are model parameters. One set of the best fitted parameters which we tried in this paper was derived by satisfying the total local surface density of $52.1 \text{ M}_\odot \text{ pc}^{-2}$ at the solar neighborhood and circular velocity $v_c(R_0) = 217 \text{ km s}^{-1}$ with $R_0 = 8 \text{ kpc}$ (Model 2 in their Table 3).

2.4.3 Discussions on Galactic potential models

Obviously most models of g_z (see Figure 2) are acceptable in the regions *only around the sun and near the mid-plane*, which can *not* be used to simulate pulsar motions farther than a few kpc from the Sun in our Galaxy. The change of acceleration (both g_z and g_R) with R and z (see Figure 3) must be considered. Previous results based on simulations with only g_z acceleration (e.g. Bhattacharya et al. 1992) therefore should be treated with caution.

An accurate model for the mass distribution and acceleration is needed for better understanding of pulsar motions in our Galaxy. The rotation curves for models of Dehnen & Binney (1998), Paczyński (1990), and Carlberg & Innanen (1987) with modified parameters by Kuijken & Gilmore (1989) are shown in Figure 4. We noticed that the potential given by Dehnen & Binney (1998) is almost the same with that by Paczyński (1990), though newer constraints were used. Our simulations for both potentials produced very similar results. The main difference between these two models is the rotation curve peak at $R \sim 300 \text{ pc}$, which Dehnen & Binney (1998) did not but Paczyński (1990) did consider the rotation curve given by Burton & Gordon (1976) in small- R

part fitted from the HI data of Westerhout (1976). Although the peak at the small- R is not unusual in spiral galaxies (Sofue et al. 1999), it is not clear whether and how the central bar affects the rotation in our Galaxy (Dehnen private communication). Therefore, in our simulations we only consider pulsar motions in the region of $0.4 \text{ kpc} < R < 25 \text{ kpc}$.

We also noticed that the mass model of Carlberg & Innanen (1987) even with modified parameters by Kuijken & Gilmore (1989) cannot produce the proper rotation curve at high z and large R . The very slow change of the potential near the Galactic center (Figure 3) is not reasonable. The accelerations given by Dehnen & Binney (1998) and Paczyński (1990) at small R and at high z (see Figure 3) seems to be better constrained by observational data (see Figure 4). Therefore the models of Dehnen & Binney (1998) and Paczyński (1990) are recommended here. Paczyński's potential is preferable due to its simple analytic form.

2.5 Governing equations and calculation method

The initial velocities and positions of the pulsars were generated randomly according to the discussions above. The rotation velocity was calculated from the Galactic potential. The motion of a pulsar is therefore only governed by the Newtonian kinetic equation as,

$$\begin{cases} \frac{d\vec{r}(t)}{dt} = \vec{v}(\vec{r}) \\ \frac{d\vec{v}(\vec{r})}{dt} = \vec{g}(\vec{r}), \end{cases} \quad (23)$$

where $\vec{r}(t)$, $\vec{v}(\vec{r})$ and $\vec{g}(\vec{r})$ are 3D vectors. The equations above were solved numerically in three directions using the 5th order Runge-Kutta method with adaptive control step-sizes [using the subroutine *rkqs*] (Press et al. 1992). The initial stepsize is $dt = 10^{-4} \text{ Myr}$, and calculations of position and velocity in 3D then continues until 0.1 Myr with adjusted stepsizes according to the required accuracy. The data are recorded every 0.1 Myr and the total energy $E_{\text{tot}} = (v_x^2 + v_y^2 + v_z^2)/2 + \phi(R, z)$ are checked. The position and velocity then are used for input of the next 0.1 Myr. The fluctuation of the total energy of each pulsar is always $< \sim 2\%$ from 0 to 2 Gyr, which we believe are good enough for simulation accuracy.

Some examples of moving trajectories of pulsars are plotted in Figure 5, with various initial conditions. Obviously, the different initial heights have very little influence on z tracks (Figure 5-A), while if the pulsar is located at different R , trajectories can be very different (Figure 5-B). Certainly, different rotation velocities (Figure 5-C) or vertical velocities (Figure 5-D) will naturally cause different trajectories.

3 RESULTS AND DISCUSSION

Limited by the computation resources available, we simulated 2×10^5 pulsars at the age $t = 0$, and put their initial positions and velocities according to the details discussed in Section 2. We then traced their motions up to an age of 2 Gyr, and perform statistics on their locations every 0.1 Myr. We first present results from Gaussian distributions of the initial height z , and Gamma-distributions for initial R ,

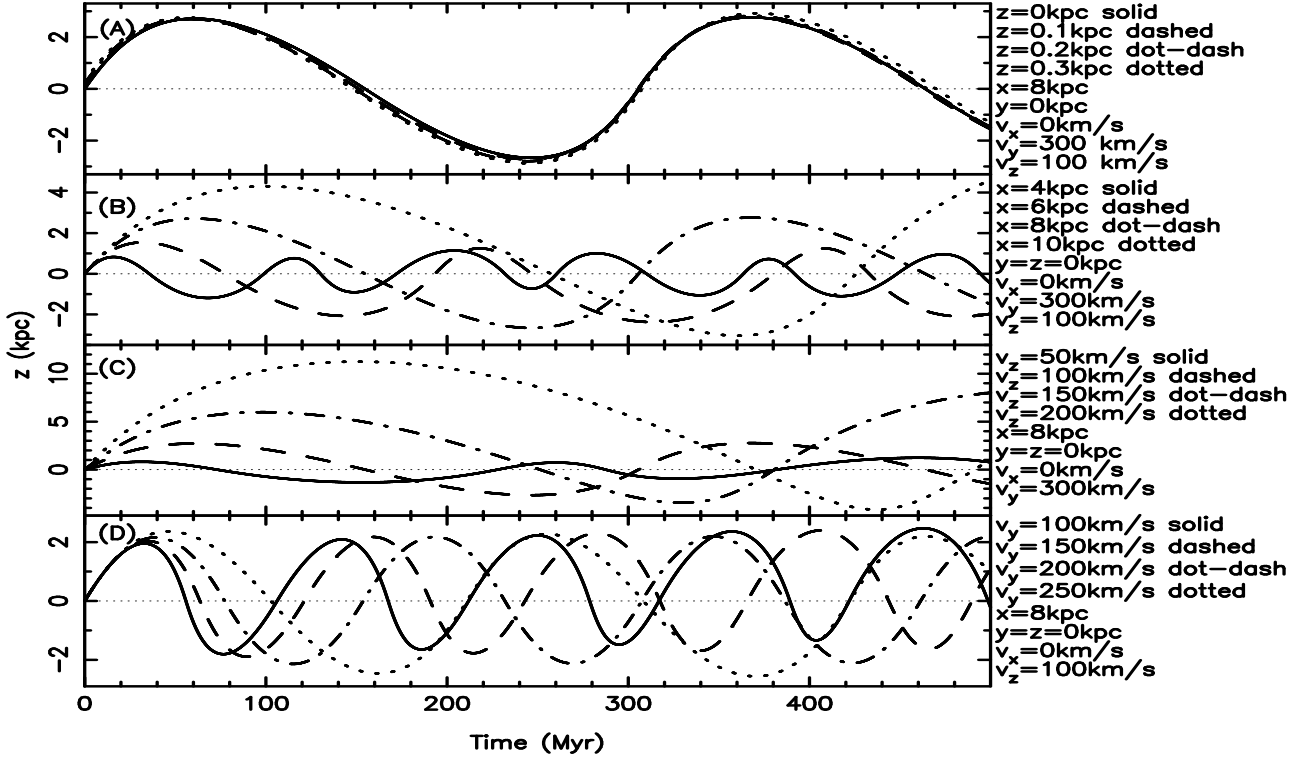


Figure 5. The z -tracks of pulsars, corresponding initial values are marked on the right side of the plots.

which will be called the standard initial conditions hereafter. We then compared those with the results from other initial conditions.

3.1 Results from standard initial conditions

3.1.1 The scale-height evolution

The z -heights of simulated pulsars are binned with equal height interval every 0.1 Myr. We used two data-sets: the average height of the i th bin, $z(i)$, and the number of pulsars in the i th bin, $N(i)$. The Levenburg-Marquardt method was then employed to fit these two data-sets with given functions (p.678 of Press et al. 1992) to obtain the height distribution.

For pulsars with an age less than 8 Myr, the height distribution can be well fitted by a single Gaussian function (Figure 6: $t=2$ Myr and 7 Myr), i.e.,

$$N(i) = A \exp\left(-\frac{z^2(i)}{2h_g^2}\right). \quad (24)$$

Here h_g is the scale-height and A is amplitude. We found that h_g increases linearly with t (Figure 7), which can be represented as

$$h_g = h_0 + \sigma t, \quad (25)$$

where h_0 and σ are fitting coefficients listed in Table 2.

The relation between σ and σ_{birth} should be discussed. At small t , one could take

$$z_t = z_{\text{ini}} + v_{\text{zini}} t \quad (26)$$

as a simplification, where z_t is height at time t . To justify this approximation, we calculated the turn-over time of pulsars, which was defined as the time when pulsars change the sign

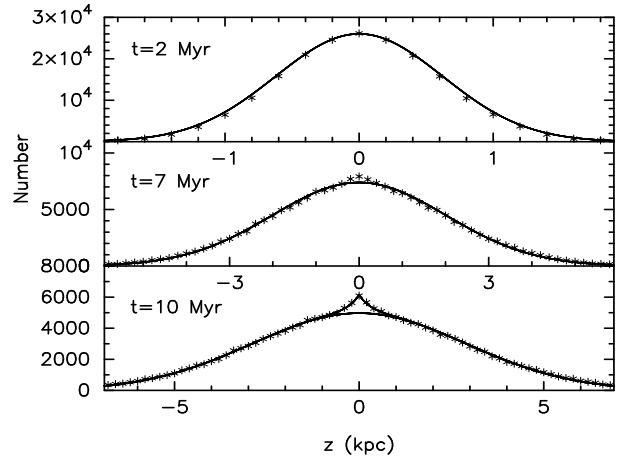


Figure 6. The height distribution can be well fitted by a Gaussian ($t < 8$ Myr) or a Gaussian plus an exponential functions ($t > 8$ Myr). Here $\sigma_{\text{birth}} = 300 \text{ km s}^{-1}$ is assumed.

Table 2. Fitting parameters for different initial 1D velocity dispersion

σ_{birth} km s^{-1}	h_0 pc	σ km s^{-1}
100	45	86
200	37	186
300	49	282
400	48	382

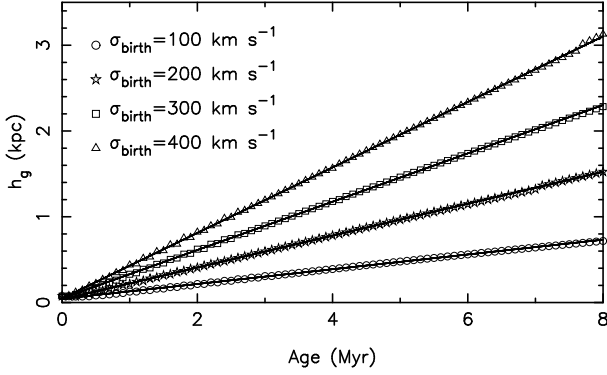


Figure 7. The scale-heights of the Gaussian components (h_g) increases linearly with ages, in spite of different birth velocities.

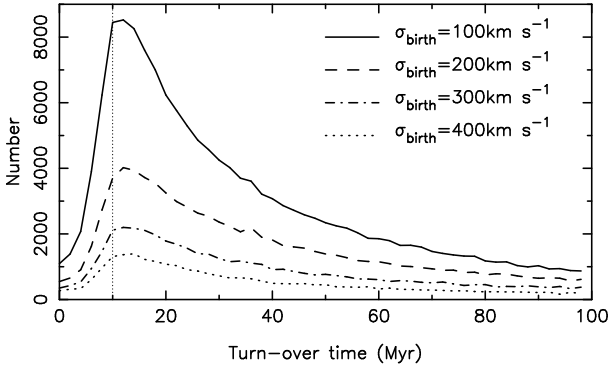


Figure 8. The distribution of pulsar turn-over times.

of v_z , i.e. start to move towards the Galactic plane for the first time. It is approximately a quarter of the oscillation period for a pulsar moving up and down. As can be seen from Figure 8, most pulsars change their motion directions (i.e. the sign of v_z) at ~ 15 Myr, a time not sensitive to initial velocities. Therefore, for a Maxwellian initial 3D velocity distribution, it is natural that the distribution of height at small age t can have a Gaussian form, and that the scale-height increases with time as $h_g \sim \sigma_{\text{birth}} t$. We noticed that roughly $\sigma_{\text{birth}} \sim \sigma$, a relation that can be used to determine 1D initial velocity dispersions. We emphasized that formula (26) is only an approximation of the first order. The effect of the deceleration of the Galactic potential did work to a certain extent, which made σ slightly smaller, i.e. $\sigma < \sim \sigma_{\text{birth}}$ (Table 2).

As time increases, the central peak in the height distribution gets more and more prominent (Figure 6: $t=10$ Myr). A single Gaussian function cannot fit the distribution satisfactorily. We found that a Gaussian plus an exponential function provides a much better fit, i.e.:

$$N(i) = A \exp\left(-\frac{z^2(i)}{2h_g^2}\right) + B \exp\left(-\frac{|z(i)|}{h_e}\right), \quad (27)$$

where h_g and h_e are scale-heights, and A and B are amplitudes. The exponential component mainly models the smaller heights and the Gaussian component accounts for the larger ones. The scale-height of Gaussian component, h_g , increases linearly with time until $t \sim 40$ Myr (Figure 9).

When $t > \sim 40$ Myr, the height distribution gets more

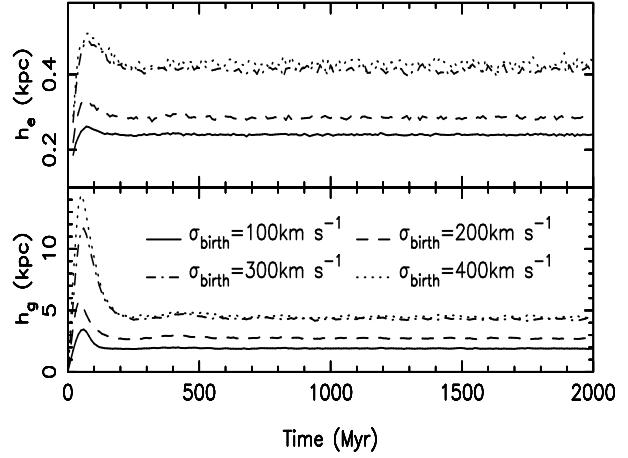


Figure 9. The evolution of the scale-heights of Gaussian component (h_g : lower panel) and exponential component (h_e : upper panel).

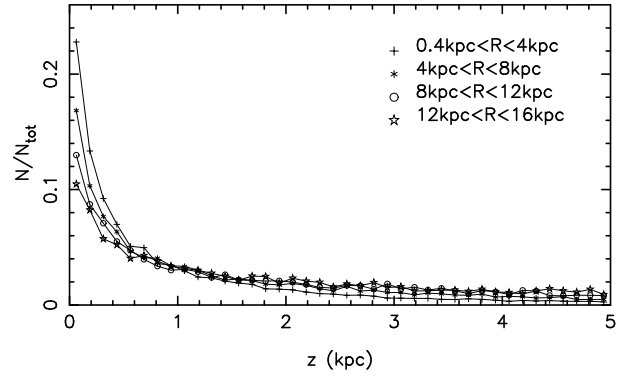


Figure 10. The height distribution at $t = 2$ Gyr in 4 R -ranges. The simulation used $\sigma_{\text{birth}} = 300 \text{ km s}^{-1}$.

concentrated towards lower heights and h_g decreases gradually (Figure 9). When $t > \sim 200$ Myr, the height distribution tends to stabilize, and both h_g and h_e show no large variations. We noticed that the larger the initial velocity dispersion, the longer the stabilization time and the larger the resulting scale-height.

3.1.2 Scale-heights at different radii

We have shown earlier that the scale-height of z distribution of all pulsars, from $0.4 \text{ kpc} \leq R \leq 25 \text{ kpc}$. It is not clear whether the z distribution changes with R .

The height distributions in four ranges of R does not show significant discrepancies (Figure 10).

3.1.3 Evolution of the radial distribution

We assume that all simulated pulsars are initially located at $0.4 \text{ kpc} < R < 25 \text{ kpc}$ with the maximum at $R = 4.5 \text{ kpc}$. During the simulation, we trace only those pulsars in the region $0.4 \text{ kpc} \leq R \leq 25 \text{ kpc}$. As mentioned above, the Galactic potential near the Galactic centre may not be realistic. This might cause exotic pulsar motion trajectories (Carlberg & Innanen 1987) so that we ignore all pulsars moving close to

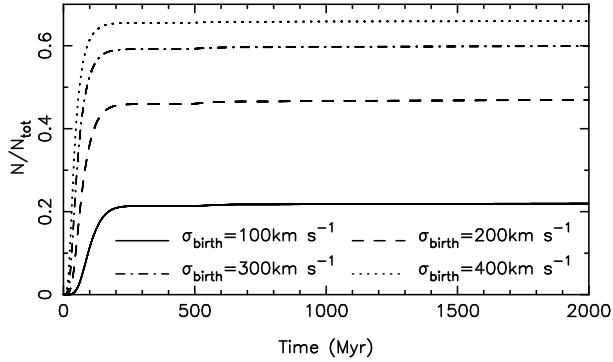


Figure 11. Fraction of the total number of pulsars that escape the Galaxy.

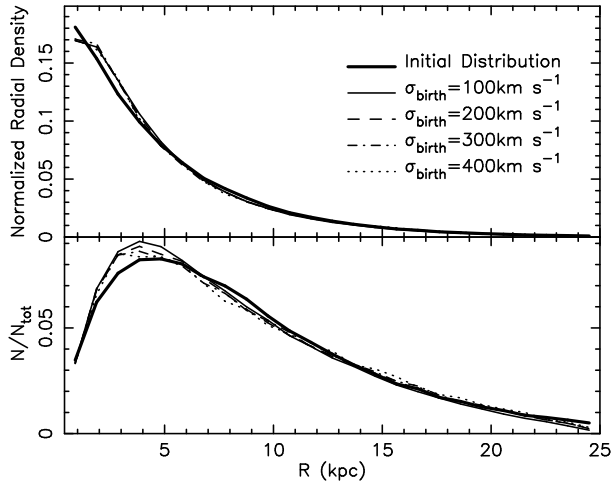


Figure 12. The R -distribution (lower panel) and the normalized radial density (upper panel) at $t=0$ (initial) and $t=2$ Gyr.

the centre ($R < 0.4$ kpc). Pulsars moving out to $R > 25$ kpc are defined as “escaped” pulsars, since the Galactic gravitation is too weak to bound them. The number of escaped pulsars increases until 200 Myr (Figure 11). The larger the initial velocities, the more likely the pulsars are to escape. For $\sigma_{\text{birth}} = 400 \text{ km s}^{-1}$, more than 60% of pulsars escape after 100 Myr. Obviously a huge amount of pulsars, even after their radio emission turns off, have gone into Galactic halo or intergalactic space, which could be a very important ingredient of the dark-matter halo.

We found that there is almost *no evolution* of the radial density and radial probability distribution (Figure 12) if the initial radial distribution is a Gamma-distribution. The different velocities do not change the distribution although numbers of remained pulsars change a lot.

Concerning the form of the radial distribution, there is a deficit towards the Galactic centre, as Johnston (1994) discussed. A peak appears at ~ 4.5 kpc, not too different from the initial distribution. However, the surface density does not have such a deficit, in contrast to the observed pulsar density distribution newly determined by Lorimer (2004).

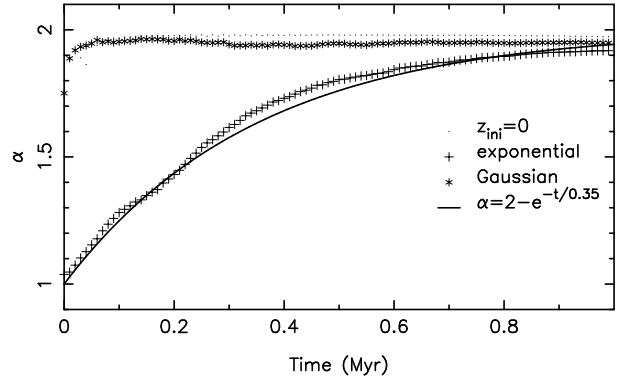


Figure 13. The change of the index α in a generalized fitting function $N(i) = A \exp\{-\left(\frac{|z(i)|}{h_\alpha}\right)^\alpha\}$.

3.2 Results for other initial conditions

3.2.1 Alternative initial height distributions

Two kinds of initial height distributions have been tried for simulations of pulsar motions: an exponential height distribution, and a flat distribution of all $z_{\text{ini}} = 0$.

For those non-Gaussian initial height distribution, a Gaussian function did not always give a good fit when $t < 1$ Myr. So we tried another function for the height distribution:

$$N(i) = A \exp\left\{-\left(\frac{|z(i)|}{h_\alpha}\right)^\alpha\right\}, \quad (28)$$

where $\alpha = 1$ corresponds to an exponential function and $\alpha = 2$ a Gaussian function. We examined a few cases of initial height distributions. As shown in Figure 13, for the initial Gaussian distribution of heights or the flat distribution with $z_{\text{ini}} = 0$, α is always nearly 2, so that we can always fix $\alpha = 2$ in the fit. For the exponential distribution of initial heights, the index α increases from 1 to 2 gradually, which can be approximately described by a function

$$\alpha = 2 - \exp\left\{-\frac{t}{0.35 \text{ Myr}}\right\}. \quad (29)$$

When t is greater than 1 Myr, the height distributions can be described by a Gaussian or a Gaussian plus an exponential function, as shown in Section 3.1.1. We therefore conclude that the pulsar height distribution is insensitive to the initial distribution after $t > 1$ Myr.

3.2.2 Alternative initial radial distributions

As we introduced in Section 2.1, alternative radial distributions can be used for simulations: (1) Gamma, (2) Gaussian, (3) offset Gaussian, (4) exponential, (5) Narayan and (6) uniform density distribution.

We first checked the evolution of height distribution, and found that all these radial distributions produce similar results, as Figure 14 shows. That is to say, the height distribution is insensitive to initial radial distribution.

The evolution of radial distributions has been checked using both the density and radial distributions (see Figure 15). Obviously pulsars at large R feel a smaller Galactic potential and hence are easy to escape after some years.

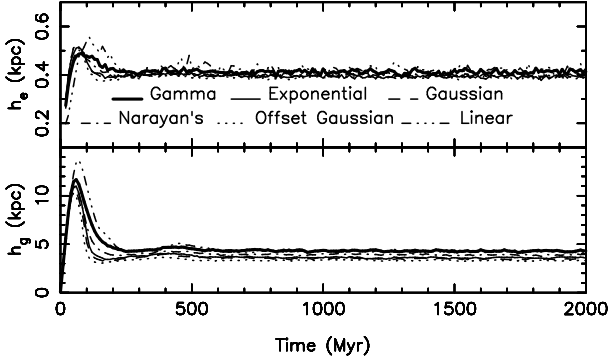


Figure 14. Evolution of scale-heights from simulations with different radial distributions.

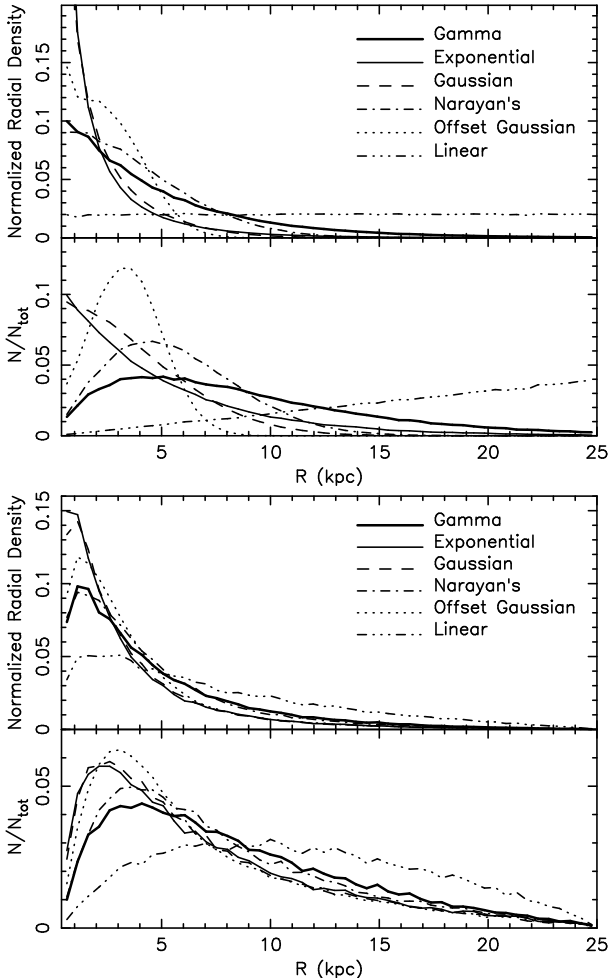


Figure 15. The density distribution (normalized ρ_R) and the radial distribution (P_R) at $t=0$ yr (upper panels) and $t=2$ Gyr (lower panels) for various initial distributions.

The final distribution seems to be more prominent at small R where the Galactic potential is much larger due to the presence of the Galactic bulge.

We indeed see the fall-off at small R in both the density distribution and radial distribution from our simulations with all kinds of initial radial distributions. However, compared to the observed deficit at small R recently determined

by Lorimer (2004), the simulated deficit is much smaller in all cases of radial distributions. Note that what we simulate simply moving neutron stars and take no account of their radio emission. It is likely that the beaming effect and the evolution of pulsar radio emission probably have to be considered carefully for a fair comparison. We can conclude from our simulation, however, that there should be a large number of evolved neutron stars near the Galactic center, which may no longer be observable as radio pulsars.

4 APPLICATIONS

All above simulations are made in ideal conditions for pulsar motions in the Galactic potential. Previous authors have simulated currently observed pulsar populations, so our results give a complementary image of pulsars moving in our Galaxy. As we just mentioned, for detailed comparison between the simulation results and observed sample, one has to consider beaming and the evolution of radio emission of pulsars. We understand that the selection effects on pulsar surveys are quite severe for a few reasons. For example, in any flux-limited survey, more luminous pulsars are easy to be detected, even they are far away. Faint pulsars can be detected only if they are very nearby. It is not clear how the luminosity of pulsars evolves with age, though evidence available shows that young pulsars tend to be brighter. Due to dispersion smearing, only nearby millisecond pulsars are easy to be discovered, mostly at high latitudes.

Nevertheless, at these two age extremes, i.e. young pulsars and millisecond pulsars, we do not have to synthesize populations for comparison of the velocity distribution or height distribution. As we do not expect the pulsar luminosity to evolve much in 1 Myr, and also previous surveys have been mostly concentrated on the Galactic plane where young pulsars live, the sample of very young pulsars suffer much less of selections effects in the surveys. For millisecond pulsars, the height distribution is very stable after 200 Myr (see Figures 9 and 14), so that millisecond pulsars of any age should follow the same height distribution fitted by a Gaussian plus an exponential function. In the following we will discuss the height distribution of young pulsars and millisecond pulsars.

4.1 Young pulsars: Initial Velocity Dispersion derived from z distribution

Most pulsar surveys have been conducted near the Galactic plane where young pulsars are predominantly found. As our simulations show, the scale-height is linearly increasing for young pulsars in the form of $h_g = h_0 + \sigma t$ for $t < 8$ Myr, which may be used to determine the initial velocity of normal pulsars.

We first take all pulsars with characteristic ages of $1 \text{ Myr} \leq \tau \leq 8 \text{ Myr}$ from the most updated pulsar catalog (Manchester et al. 2004) [¶]. Pulsar distances are estimated by using the new electron density model of NE2001 (Cordes & Lazio 2002). To make the consistency with $R_0 = 8 \text{ kpc}$, all distances have been scaled with a factor

[¶] <http://www.atnf.csiro.au/research/pulsar/catalogue/>

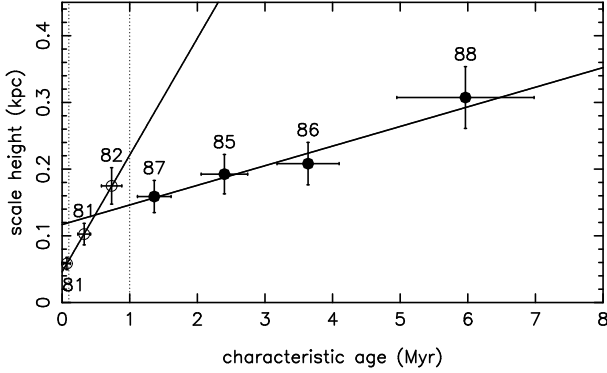


Figure 16. The scale-heights versus characteristic ages of currently known pulsars. Solid lines represent linear fits. The numbers of pulsars in the corresponding bins are indicated in the plot.

of $8/8.5=0.94$. We binned these pulsars into four groups according to their characteristic ages and obtained the scale-height h_g of each group through Gaussian fitting (filled circles in Figure 16). We then checked the relation between h_g and ages, assuming that the true age t is equal to the characteristic age τ . The resulting 1D velocity dispersion is $29 \pm 12 \text{ km s}^{-1}$, too small compared with previous results of several hundreds from proper motion measurement analyses (e. g. Lyne & Lorimer 1994; Hansen & Phinney 1997). This indicates strong selection effects in the assembled pulsar sample, as we justify below.

For young pulsars ($t < 8 \text{ Myr}$), $z = z_{\text{ini}} + v_{z\text{ini}}t$. If $z_{\text{ini}} < \sim 0.06 \text{ kpc}$ is ignored, a pulsar with z -velocity of 400 km s^{-1} will reach 0.4 kpc at 1 Myr , but 4 kpc at 10 Myr . Previous pulsar surveys, like the Parkes multibeam survey which discovered about half of all known pulsars, mainly covered $|b| \leq 5^\circ$. If the average pulsar distance is about 6 kpc , all pulsars of $|b| \leq 5^\circ$ would have a $|z| < 0.5 \text{ kpc}$ at or nearer than this average distance. Only pulsars with $\tau < 8 \text{ Myr}$ and a z -velocity less than $v_{z\text{ini}} \approx z/t = 0.5 \text{ kpc}/8 \text{ Myr} = 63 \text{ km s}^{-1}$ can be picked up in such a survey. The detected older pulsars must have much smaller z -velocities, otherwise it have to be much farther away than a distance of 6 kpc .

Pulsars younger than 1 Myr cannot move too far away even with a large initial z -velocity because of their small ages. As a result, the combined sample would not suffer much selection effects due to survey regions. This is why Lyne & Lorimer (1994) chose 1 Myr as the cut-off age of the sample. Now we try to use much more pulsars of $t < 1 \text{ Myr}$ to estimate z -velocity. About 244 pulsars have been divided into three bins, with roughly the same number of pulsars each. The 1D velocity dispersion in z direction derived from the scale-heights of z distributions of three sub-samples is $175 \pm 56 \text{ km s}^{-1}$, as shown in Figure 16. This corresponds to a 3D velocity dispersion of $303 \pm 97 \text{ km s}^{-1}$ or a mean velocity of $280 \pm 96 \text{ km s}^{-1}$.

To compare with previous estimates of velocities, we should use Taylor & Cordes (1993) model for pulsar distance, and should not include the pre-scaling factor from R_0 . We then found the 1D velocity dispersion of $187 \pm 64 \text{ km s}^{-1}$, or a 3D velocity dispersion of $324 \pm 110 \text{ km s}^{-1}$ and the mean velocity of $299 \pm 102 \text{ km s}^{-1}$. These values are consistent with estimates given by Hansen & Phinney (1997), the mean pul-

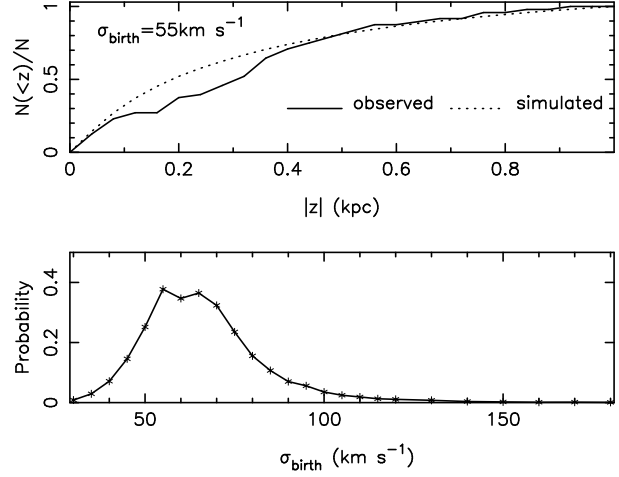


Figure 17. K-S test: Cumulative probability distributions of simulated and observed samples (upper panel), and the significance level for different initial velocities (lower panel).

sar velocity of 250 km s^{-1} , or by Lyne & Lorimer (1994), the mean of $450 \pm 90 \text{ km s}^{-1}$.

4.2 Initial Velocity Dispersion of MSPs

MSPs have a more complex evolutionary history than normal pulsars. Generally, MSPs are old neutron stars spun up by mass and momentum transferring from the companions (e.g. Alpar et al. (1982)). Their “birth” velocity is either the velocity of the binary system or its sole velocity after the disruption of the binary system. Another consecutive problem is their ages. Characteristic ages from period and period derivative probably do not reflect their true ages. Are they chronologically old? Hansen & Phinney (1997) demonstrated that pulsars older than 10^7 yr show the asymmetric drifts. Toscano et al. (1999) confirmed the asymmetric drifts of MSPs, which justify that MSPs are really dynamically old enough to be virialized. There is no doubt that MSPs are really old objects in the Milky Way.

From our simulation, the height distribution of old pulsars (e.g. $t > 200 \text{ Myr}$) is stabilized. MSPs of all ages follow the same height distribution. For the comparison of z -distributions of simulated sample and observed sample, we did not take into account selection effects for the MSP discovery. The observed sample consists of 48 MSPs from the latest pulsar catalog after discarding the MSPs in globular clusters. The simulated sample are old pulsars within 3 kpc from the Sun in a number of sets of simulations with initial 1D z -velocity dispersion from 30 km s^{-1} to 180 km s^{-1} (with a step of 5 km s^{-1}). The K-S test is employed to check whether these two distributions are from the same parent distribution. We find that $\sigma_{\text{birth}} = 60 \pm 10 \text{ km s}^{-1}$ gives the largest probability. If the velocities of MSPs follow a Maxwellian distribution, the 1D velocity dispersion is most probably $60 \pm 10 \text{ km s}^{-1}$ or the mean velocity dispersion most probably $96 \pm 16 \text{ km s}^{-1}$, consistent with previous results (e.g. Lyne et al. 1998).

5 CONCLUSIONS

We presented a generalized statistical picture of how pulsars move in our Galaxy. The potential given by Paczyński (1990) can be a good representation of mass distribution of our Galaxy, and has a simple analytic formula. We found that the final height distributions are not sensitive to the forms of initial z and R distributions. The height distribution can be well fitted by a Gaussian function within ~ 8 Myr, and the scale-height increases linearly with time. After that an extra exponential function is required to fit the height distribution. The height distribution gets stabilized after about 200 Myr.

The height distribution of pulsars younger than 1 Myr implies directly that the mean initial velocity of 280 ± 96 km s $^{-1}$. Comparison of the simulated sample of millisecond pulsars and observed sample suggests the 1D initial velocity dispersion of MSPs to be most probably 60 ± 10 km s $^{-1}$, consistent with estimates given by previous authors.

ACKNOWLEDGMENTS

We would like to thank the referee, Dr. Dunc Lorimer, for very detailed comments and suggestions, which led to significant improvements of the paper. We thank Prof. Andrew Lyne for valuable discussions and Drs. Walter Dehnen and Xianghua Li for their patient help on software. This work is supported by the National Natural Science Foundation of China (19903003 and 10025313) and the National Key Basic Research Science Foundation of China (G19990754) as well as the partner group of MPIfR at NAOC.

REFERENCES

- Alpar M. A., Cheng A. F., Ruderman M. A., Shaham J., 1982, *Nat.*, 300, 728
- Arnaud M., Rothenflug R., 1981, *A&A*, 103, 263
- Arzoumanian Z., Chernoff D. F., Cordes J. M., 2002, *ApJ*, 568, 289
- Bahcall J. N., 1986, *ARA&A* 24, 577
- Bailes M., Kniffen D. A., 1992, *ApJ*, 391, 659
- Bhattacharya D., Wijers R. A. M. J., Hartman J. W., Verbunt F., 1992, *A&A*, 254, 198
- Burton W. B., Gordon M. A., 1978, *A&A*, 63, 7
- Carlberg R., Innanen K., 1987, *AJ*, 94, 666
- Cordes J. M., Chernoff D. F., 1997, *ApJ*, 482, 971
- Cordes J. M., Chernoff D. F., 1998, *ApJ*, 505, 315
- Cordes J. M., Lazio T. J. W., 2002, in press, *astro-ph/0207156*
- Dehnen W., Binney J., 1998, *MNRAS*, 294, 429
- Dewey R. J., Cordes J. M., 1987, *ApJ*, 321, 780
- Ferrière K., 1998, *ApJ*, 497, 759
- Gonthier P. L., Ouellette M. S., Berrier J. et al., 2002, *ApJ*, 565, 482
- Gunn J. E., Ostriker J. P., 1970, *ApJ*, 160, 979
- Hansen B.M.S., Phinney E.S., 1997, *MNRAS*, 291, 569
- Hartman J. W., Bhattacharya D., Wijers R., Verbunt F., 1997, *A&A*, 322, 477
- Hartman J. W., Verbunt F., 1995, *A&A*, 296, 110
- Helfand D. J., Tadamaru E., 1977, *ApJ*, 216, 842
- Itoh N., Hiraki K., 1994, *ApJ*, 435, 784
- Johnston S., 1994, *MNRAS*, 268, 595
- Kuijken K., Gilmore G., 1989, *MNRAS*, 239, 571, 605
- Lorimer D. R., 1995, *MNRAS*, 274, 300
- Lorimer D. R., 2004, In: F. Camilo & B. M. Gaensler, eds., *IAU Symposium*, Vol. 218, *Young Neutron Stars and Their Environments*.
- Lorimer D. R., Bailes M., Dewey R. J., Harrison P. A., 1993, *MNRAS*, 263, 403
- Lorimer D. R., Bailes M., Harrison P. A., 1997, *MNRAS*, 289, 592
- Lyne A. G., Lorimer D.R., 1994, *Nat*, 369, 127
- Lyne A. G., Manchester R. N., Lorimer D. R. et al., 1998, *MNRAS*, 295, 743
- Lyne A. G., Manchester R. N., Taylor J. H., 1985, *MNRAS*, 213, 613
- Maíz-Apellániz J., 2001, *AJ*, 121, 2737
- Manchester R. N., Hobbs, G., Teoh, A., Hobbs, M., 2004, In: F. Camilo & B. M. Gaensler, eds., *IAU Symposium*, Vol. 218, *Young Neutron Stars and Their Environments*.
- Mihalas D., Binney J., 1981, *Galactic Astronomy* (San Francisco: Freeman)
- Miyamoto M., Nagai R., 1975, *PASJ*, 27, 533
- Mukherjee S., Kembhavi A., 1997, *ApJ*, 489, 928
- Narayan R., 1987, *ApJ*, 319, 162
- Narayan R., Ostriker J. P., 1990, *ApJ*, 352, 222
- Paczyński B., 1990, *ApJ*, 348, 485
- Press W. H., Teukolsky S. A., Vetterling W. T., Flannery B. P., 1992, *Numerical Recipes in Fortran*, Second edition. p.705
- Sofue Y., Rubin V., 2001, *ARA&A* 39, 137
- Sofue Y., Tutui Y., Honma M. et al., 1999, *ApJ*, 523, 136
- Taylor J. H., Cordes J. M., 1993, *ApJ*, 411, 674
- Toscano M., Sandhu J. S., Bailes M. et al., 1999, *MNRAS*, 307, 925
- Westerhout G.: 1976, *Maryland-Bonn Galactic 21-cm Line Survey*, University of Maryland, College Park.